Odd-parity effect and scale-dependent viscosity in atomic quantum gases

Check for updates

Jeff Maki [1,2] ✉, Ulf Gran [3] ✉ & Johannes Hofmann [4,5] ✉

Two-dimensional electron gases are predicted to possess an anomalous "tomographic" transport regime that is marked by an odd-even effect in the relaxation times, with odd-parity deformations of the Fermi surface becoming long-lived in comparison to even-parity ones. In this work, we establish that neutral two-component atomic Fermi gases also exhibit this tomographic effect. By diagonalizing the Fermi liquid collision integral, we identify odd-parity modes with anomalously long lifetimes below temperatures $T \leq 0.15 T_F$, which is within reach of cold atom experiments. Furthermore, in contrast to electron gases, we find that the odd-even effect in neutral gases is widely tuneable with interactions along the BCS-BEC crossover and is suppressed on the BEC side. We propose as an experimental signature of the odd-even effect the damping rate of quadrupole oscillations, which is anomalously enhanced due to the presence of long-lived odd-parity modes. Our findings suggest that the dynamics of two-dimensional Fermi gases is richer than previously thought and should include additional long-lived modes.

Thermodynamic and transport properties of the normal state of metals as well as ^{3}He are well described by a semiclassical Fermi gas model[1,2]. The microscopic justification of this surprisingly simple description, despite nominally strong interactions, is provided by Landau's theory of the Fermi liquid[3,4], which describes thermodynamic and transport properties in terms of a collection of weakly interacting quasiparticles[5–7]. The validity of this picture relies on the presence of a Fermi surface and concomitant Pauli blocking, which strongly restricts the available phase space for quasiparticle scattering, leading to well-defined quasiparticles with lifetimes that diverge quadratically at low temperatures, $\tau \sim 1/T^2$. In recent years, Fermi liquid theory has also been applied to a variety of ultracold quantum gas setups, such as minority polarons in strongly spin-imbalanced Fermi gases[8–11], the normal phase of balanced Fermi gases above the superfluid transition[12–15], transport and collective modes[16] and even few-body systems[17]. For transport measurements, quasiparticle interactions lead to internal dissipative processes with relaxation times that set the magnitude of transport coefficients like the shear viscosity. The general expectation is that these transport times are equal to the quasiparticle lifetimes.

Recent theoretical work in the context of interaction-dominated electron gases in two dimensions has provided evidence to the contrary and indicates the existence of deformations of the Fermi surface that have significantly longer lifetimes[18–22]: Indeed, a standard Fermi liquid scaling $\tau_e \sim 1/T^2$ is argued to only apply to a subclass of collective quasiparticle deformations—dubbed even-parity modes—while the remaining modes—dubbed odd-parity modes—decay significantly more slowly as $\tau_o \sim 1/T^4$. This leads to the exciting perspective that, at low temperatures, these long-lived modes impact the hydrodynamic description of the gas (in addition to modes that are linked to conserved currents and have infinite lifetime), such that the transport properties of Fermi liquids become richer than commonly assumed. For this reason, there is now intense effort to identify experimental signatures of odd-parity transport, or "tomographic transport", in electron Fermi liquids[19,23–27]. Quite generally, an isolated odd-parity response that is not dominated by even-parity modes appears in transverse probes at finite wavelengths, such as the transverse conductivity[19] or transverse collective modes[23]. However, it has so far not been possible to detect such transverse probes in electron Fermi liquids, while in ^{3}He, measurements of transverse sound have been inconclusive[28,29]. By contrast, quantum gases offer an entirely separate way of inducing transverse dynamics by manipulating the real-space confinement of an external trap. Moreover, since on a microscopic level the odd-even effect is linked to the Fermi statistics and Pauli blocking, one should expect (and as we confirm theoretically) that this effect is not only present for electron gases but also in charge-neutral Fermi liquids. The purpose of this work is thus to initiate a search for the odd-even effect in neutral quantum gases.

The key results of our work, illustrated in Fig. 1, are twofold: first, we establish that, just as for electron gases, an enhancement in the lifetime of

^{1}Department of Physics, University of Konstanz, Konstanz, Germany. ^{2}Pitaevskii BEC Center, CNR-INO and Dipartimento di Fisica, Università di Trento, Trento, Italy. ^{3}Department of Physics, Chalmers University of Technology, Gothenburg, Sweden. ^{4}Department of Physics, Gothenburg University, Gothenburg, Sweden. ^{5}Nordita, Stockholm University and KTH Royal Institute of Technology, Stockholm, Sweden. ✉e-mail: jeffrey.maki@uni-konstanz.de; ulf.gran@chalmers.se; johannes.hofmann@physics.gu.se
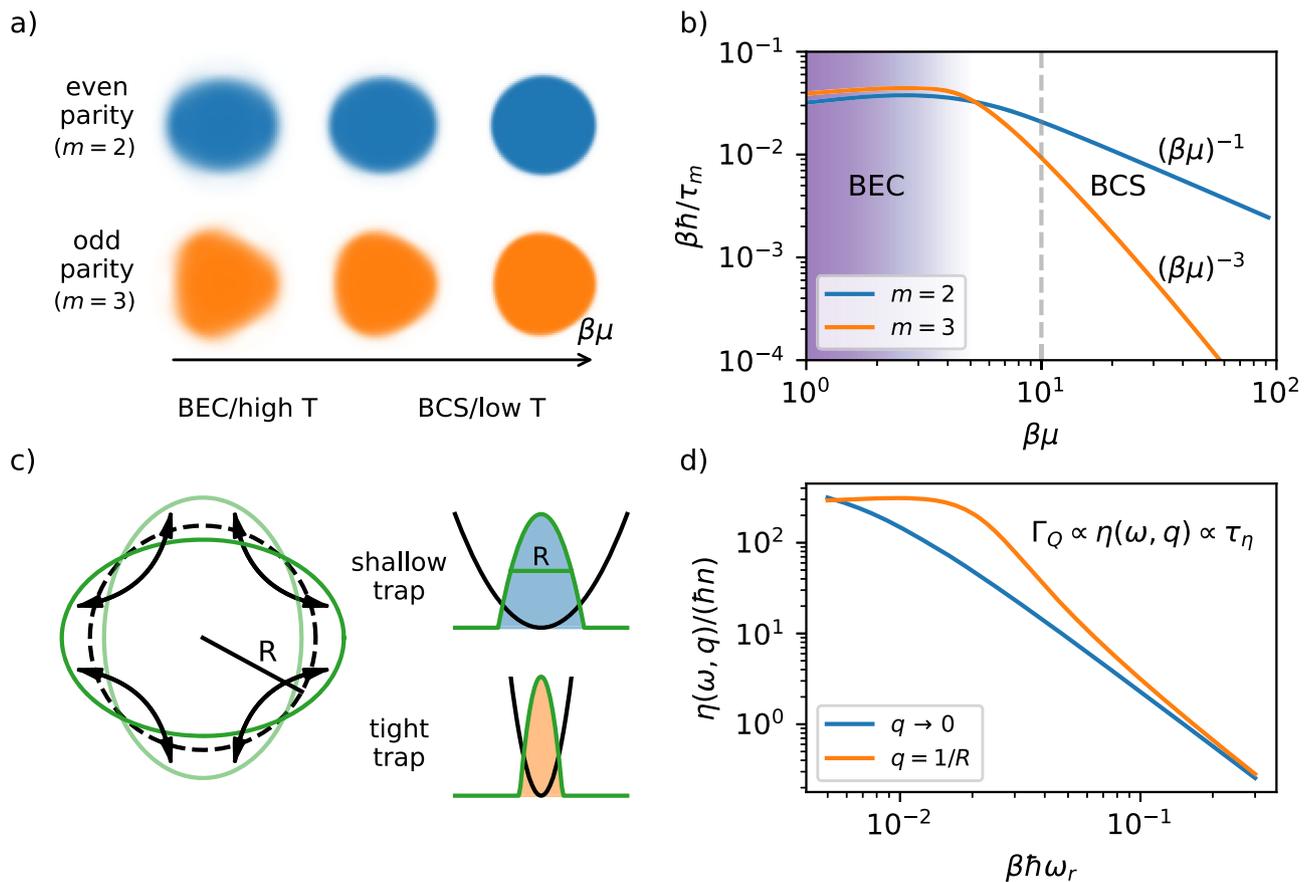
Fig. 1 | Tomographic transport in atomic gases. a Nonequilibrium momentum-space distribution for different temperatures T (where $\beta = 1/[k_B T]$ is the inverse temperature and k_B is the Boltzmann constant) and **b** dimensionless relaxation rates $\beta\hbar/\tau_m$ of the first collective even-parity Fermi surface deformation with angular momentum $m = 2$ (blue) and the first collective odd-parity deformation with $m = 3$ (orange). Even (odd) parity refers to an equal (opposite) deformation of the distribution at opposite momenta. With decreasing temperature and increasing density (i.e., increasing $\beta\mu$, where μ is the chemical potential), the equilibrium Fermi surface becomes sharper, and Pauli blocking diminishes the available phase space for scattering, increasing the lifetime of the modes. The conventional Fermi liquid relaxation rate $\sim T^2/\mu$ of the even-parity mode is set by an angular redistribution on the Fermi surface of pairs with equal and opposite momenta. Such a process does not relax the odd-parity modes, however, which have a significantly slower relaxation rate $\sim T^4/\mu^3$. For interacting Fermi gases along the BCS-BEC crossover, the discrepancy of odd and even-parity lifetimes is present on the BCS side of the crossover,

for which the chemical potential is positive, $\beta\mu > 0$ (the gray dashed line indicates the non-interacting chemical potential at a moderately small temperature $T/T_F = 0.1$ for reference). The effect is then reduced with increasing pairing interaction and vanishes on the BEC side where $\beta\mu < 0$. **c** Real-space dynamics and **d** damping rate Γ_Q as a function of trap frequency ω_r of the quadrupole mode in a harmonic trap. The quadrupole mode oscillates with frequency $\omega_Q = \sqrt{2}\omega_r$ and involves a shear flow in real space. The real-space density profile is shown in the insets and sets the equilibrium size R. The damping rate of the quadrupole mode is controlled by the shear viscosity spectral function $\eta(\omega, q)$, which is proportional to the relaxation time of a collective shear deformation of the Fermi surface in momentum space. In a bulk system (shallow trap), this deformation corresponds to the hydrodynamic even-parity mode with $m = 2$, but at finite confinement, odd-parity modes contribute, and the increased odd-parity lifetime leads to an increased damping rate (orange line) compared to the hydrodynamic prediction (blue line). This damping provides evidence of the enhanced odd-parity lifetime.

odd-parity deformations of the Fermi surface also exists for neutral atomic Fermi quantum gases [Fig. 1a]. From an exact diagonalization of the linearized kinetic collision integral (see methods), we find that these lifetimes differ significantly within temperature ranges accessible in current cold atom experiments [Fig. 1b]. Moreover, in a marked difference from electron gases, we demonstrate that the effect is widely tunable with interaction strength along the BCS-BEC crossover and vanishes near resonance and on the BEC side of the crossover where the chemical potential μ is negative and the Fermi surface disappears. As a second key result, we propose as an experimental signature of the odd-even effect the damping rate of collective quadrupole oscillations in a harmonic trap, which involve a shear flow of atoms in real space [Fig. 1c]. The damping rate of the oscillations is governed by the shear viscosity, which is evaluated at a finite wavenumber set by the trap curvature. As discussed above, this implies that the damping rate is proportional to the relaxation time of the momentum space deformation that is induced by the shear flow in the harmonic trap, $\eta \approx n p_F v_F \tau_\eta$. For a shallow trap, the standard hydrodynamic result for the shear viscosity involves an even-parity deformation

with conventional Fermi liquid lifetime, while for larger confinements, odd-parity modes dominate. Since the shear viscosity is related to the lifetime of a deformation of the Fermi surface induced by the shear flow, the reduced scattering of the odd-parity modes translates to an anomalously enhanced shear viscosity at finite wavenumber and hence an increased damping rate of the quadrupole mode when odd-parity modes become relevant. Indeed, a full evaluation of the momentum- and frequency-dependent shear viscosity spectral function [Fig. 1d] shows a strong increase of the damping rate compared to the hydrodynamic prediction for intermediate trap frequencies ω_r and realistic system parameters. Moreover, as will be discussed below, the effect is enhanced even further both at low temperatures and for small atom numbers, i.e., for mesoscopic Fermi gases. Overall, these findings imply that in experiments with cold gases, the odd parity effect can be widely tuned in a characteristic manner with interaction strength, temperature, harmonic trap frequency, and particle number. Ultracold Fermi gases are thus an ideal platform to study the anomalous relaxation dynamics of collective modes, and it should be readily possible to establish the odd-even effect in the

quasiparticle lifetimes by comparing the damping of the quadrupole mode at different experimental parameter values.

Results

Quasiparticle lifetimes

We first establish the odd-even effect in the lifetimes of the odd and even parity modes of the quasiparticle distribution at low temperatures on the BCS side of the normal region of the BCS-BEC crossover (where a well-defined Fermi surface exists) and show that it vanishes along the crossover. Intuitively, this is linked to the fact that fermions along the crossover form increasingly tightly bound dimers, which reduces the chemical potential and destroys the Fermi surface, and with it the Pauli blocking that is at the heart of the odd-even effect. For 2D atomic gases, interactions are short-ranged and described by a delta-function with strength $\hbar^2 \tilde{g}/m^*$ with a dimensionless parameter $\tilde{g} = -2\pi/\ln(k_F a_2)$, where k_F is the Fermi wavevector, m^* is the mass of the atoms and a_2 is the 2D scattering length. At a given temperature and density, the interactions interpolate between the BCS side [$\tilde{g} < 0$ or $\ln(k_F a_2) > 0$] and the BEC side [$\tilde{g} > 0$ or $\ln(k_F a_2) < 0$], tuned by either Feshbach[30] or confinement-induced resonances[31].

The fundamental quantities to describe are the relaxation rates of collective deviations in the quasiparticle distribution from local equilibrium (which is given by a Fermi-Dirac distribution $n_{FD}(\mathbf{p})$). These relaxation rates are defined as the eigenvalues of the linearized collision integral (see methods),

$$\mathcal{L}[\psi_m(\mathbf{p})] = -\frac{1}{\tau_m}\psi_m(\mathbf{p}), \qquad (1)$$

where the eigenvalue $1/\tau_m$ is the relaxation rate and the eigenfunction $\psi_m(\mathbf{p})$ parameterizes a collective quasiparticle deviation as

$$\begin{aligned}\delta n(\mathbf{p}) &= n(\mathbf{p}) - n_{FD}(\mathbf{p}) \\ &= n_{FD}(\mathbf{p})(1 - n_{FD}(\mathbf{p}))\,\psi(\mathbf{p}).\end{aligned} \qquad (2)$$

Due to the rotational invariance of the system, the eigenmodes ψ_m carry a definite angular momentum quantum number $m = 0, \pm 1, \pm 2, \ldots$. Modes with even (odd) m have even (odd) parity [see Fig. 1a]. An additional radial quantum number (not indexed explicitly here) describes the number of radial nodes in the eigenfunction, with faster relaxation (i.e., larger $1/\tau_m$) for modes with increasing node number[21]. Due to conservation of particle number, energy, and momentum, the lowest eigenvalues with $m = 0$ and $m = \pm 1$ are zero. The leading finite even-parity mode has then angular momentum $m = \pm 2$ while the leading odd-parity mode has angular momentum $m = \pm 3$[21]. The corresponding momentum space deformations are shown in Fig. 1a for three different temperatures. The $m = 2$ mode sets the dominant contribution to the hydrodynamic shear viscosity[32-34], while the second mode will give the leading correction in a finite trap geometry and induce the anomalous enhancement of the damping rate.

Figure 1b shows results for the smallest finite relaxation rates τ_m with odd and even parity, where we use the expansion method developed in refs. 20,21 to determine the eigenvalues of the collision integral to arbitrary precision. The key observation is the parity-dependence of the lifetime at large $\beta\mu$ ($\beta = 1/[k_B T]$ and k_B is Boltzmann's constant), where Pauli blocking leads to a different scaling of the odd- and even-lifetimes with chemical potential and temperature: odd modes scale as $\beta^4\mu^3$, while even modes scale as $\beta^2\mu$ [indicated in Fig. 1b]. Current experiments reach $T/T_F \approx 0.1 - 0.5$[14,35-38], which is indicated by the dashed gray line in Fig. 1b for the BCS limit, for which the chemical potential is approximately that of a non-interacting Fermi gas. Already at this point the odd and even lifetimes differ by a factor of two, and even a minor further decrease in temperature (i.e., larger $\beta\mu$) will significantly enhance the odd-even effect: For example, for $T/T_F \approx 0.05$ the odd and even lifetimes differ by one order of magnitude. On the BEC side [purple shaded area in Fig. 1b], the chemical potential becomes negative, $\beta\mu < 0$, and scales with the binding energy $\epsilon_b = 1/(m^* a_2^2)$ of the two-body bound state, $\mu = -\epsilon_b/2$. In this regime, odd and even relaxation times are approximately

equal and scale as $\tau_m \sim e^{-\beta\mu}$. As discussed, intuitively on the BEC side there is no well-defined Fermi surface and thus one expects the odd-even effect to vanish. This result implies that the odd-even effect is tuned not only by changing the temperature but also the interaction strength. Since the odd-even effect is due to the kinematic constraints of low-energy scattering in the presence of a Fermi surface, it is not overly sensitive to the structure of the two-particle matrix element in the collision integral[18,20]. We have confirmed this by considering various approximations for the two-body scattering matrix, see Supplementary Note I for details.

Shear viscosity

We now propose to observe the odd-even effect along the BCS-BEC crossover by examining the transverse collective dynamics of the gas in real space. In atomic gases, a transverse flow is induced by collective quadrupole modes, which are anisotropic oscillations of a harmonically trapped quantum gas[14,35,39-47]. This is shown schematically in Fig. 1c alongside the radial equilibrium density distribution for the Fermi gas for different trap confinements, which at low temperatures is a Thomas-Fermi profile with radius $R = \hbar k_F/(m^*\omega_r) = \sqrt{2\hbar\sqrt{N}/(m^*\omega_r)}$. The quadrupolar flow is incompressible and there is no change in the internal energy[14,39-41]. This yields an oscillation frequency that is independent of the equation of state in the strongly interacting limit, $\omega_Q = \sqrt{2}\omega_r$,[14] where ω_r is the frequency of the harmonic trap. In general, the frequency of the quadrupole mode depends on the interaction strength and scales as $\omega_Q = \sqrt{2(2 + \tilde{g})/(1 - \tilde{g})}\omega_r$ in the collisionless limit[39]. However, this change in the frequency does not qualitatively affect our analysis, which relies primarily on the finite wavenumber q.

The damping rate Γ_Q of the quadrupole mode is linked to the local shear viscosity spectral function evaluated at the quadrupole mode frequency, $\eta(\omega_Q, \mathbf{r})$, via[14,35,42-45]

$$\Gamma_Q = E_{\text{kin},Q}^{-1} \int d\mathbf{r}\,\eta(\omega_Q, \mathbf{r})\frac{1}{2}\left(\partial_x \mathbf{v}_Q^y + \partial_y \mathbf{v}_Q^x\right)^2. \qquad (3)$$

In this expression, $E_{\text{kin},Q} = \int d\mathbf{r}\frac{m^*}{2}\mathbf{v}_Q^2 n(\mathbf{r})$ is the kinetic energy associated with the quadrupolar velocity field $\mathbf{v}_Q = b(y\hat{x} + x\hat{y})$ (b is a constant with units of frequency), and the density of the gas in the harmonic trap $n(\mathbf{r})$ is evaluated in the local density approximation [see Fig. 1c]. The shear viscosity is then a local quantity that also depends on the characteristic frequency. The wavenumber dependence of the shear viscosity spectral function encodes the odd-even effect and the anomalously long-lived odd-parity modes. Seen in Fourier space, the integral over space in Eq. (3) is equivalent to a trap average that selects a finite dominant wavenumber q at which the density $n(\mathbf{r})$ and current $n(\mathbf{r})\mathbf{v}_Q$ vary during the quadrupole motion. At low temperatures, the density profile is a Thomas-Fermi distribution, and the relevant momentum scale is set by the inverse of the Thomas-Fermi radius; $q \sim 1/R$. The damping rate of the quadrupole mode after trap averaging is then $\Gamma_Q \sim \eta(\omega_Q, q)$, which in turn is a measure of the relaxation time of shear deformations in momentum space.

In the limit of very shallow harmonic traps, the system is nearly homogeneous and the damping rate is related to the shear viscosity spectral function at $q = 0$. This is the hydrodynamic limit that is dominated by the relaxation of the even-parity $m = \pm 2$ mode[32-34]. At finite trap frequencies, i.e., for finite trap curvature $q \sim 1/R$, the odd-parity modes ($m = \pm 3$ and higher angular momenta) contribute. To obtain an estimate of the characteristic parameter scales at which these odd-parity modes become relevant, we use a relaxation time approximation with a single characteristic even (odd) parity modes decay rate γ_e (γ_o). At low temperatures, these relaxation rates scale as $\gamma_e \sim \tilde{g}^2 T^2/T_F$ and $\gamma_o \sim \tilde{g}^2 T^4/T_F^3$[19-21]. When the odd-even effect is present $\gamma_e \gg \gamma_o$, there is an emergent length scale that defines the tomographic transport limit $\xi = v_F/\sqrt{\gamma_e\gamma_o}$, where for $q\xi \sim 1$ the system is in the tomographic transport regime, while for $q\xi \ll 1$ is the hydrodynamic regime. In the presence of a harmonic trap, both the relevant wavenumber

$q \sim \sqrt{\omega_r}/N^{1/4}$ and frequency $\omega_Q = \sqrt{2}\omega_r$ are set by the harmonic trap frequency ω_r and the atom number N. Hence, by tuning the trap frequency we explore the shear viscosity spectral function on a line in the $\{\omega, q\}$ parameter space. Expressed in terms of the trap frequency, the condition $q\xi \sim 1$ to observe the odd-even effect in a harmonic trap translates to

$$q\xi \sim \frac{N\omega_r^3}{\tilde{g}^2 T^3} \sim 1, \tag{4}$$

implying that the odd-even effect will be important for $\omega_r \sim \tilde{g}^2 T^3/N$.

In Fig. 1d, we compare the results for the shear viscosity at finite and zero momentum for $T/T_F = 0.1$ following the Fermi liquid approach outlined in the methods section and Supplementary Note II. Already for intermediate trap sizes, we see a noticeable difference between the hydrodynamic and finite momentum predictions, which indicates a significant enhancement of the damping rate compared to the hydrodynamic prediction that is due to the anomalous increase in the lifetime of odd-parity modes.

For further illustration, Fig. 2a shows a spectral plot of the shear viscosity spectral function at finite frequency and momentum as obtained using a Fermi liquid two-body scattering matrix element, where we extract the Landau parameters from experimental data on the low-temperature equation of state[37]. In general, the shear viscosity spectral function is related to the retarded correlation function of the off-diagonal elements of the stress tensor[48], the poles of which give the transverse collective modes. However, in our case the transverse sound pole is diffusive, as the transverse sound mode

only becomes real when $F_1 > 1$[49]. At zero momentum and finite frequency, we find that the spectral function has a Lorentzian shape that describes the standard hydrodynamic-to-collisionless crossover[42–44]. At finite momentum, the shear viscosity spectral function vanishes at small frequencies, which reflects the fact that the fluid responds instantaneously to the transverse velocity field. At large frequencies the shear viscosity is known to decay as ω^{-2} in the collisionless limit[32]. Hence one observes a local maximum in the shear viscosity spectral function at finite momentum. The trajectory $(q, \omega) = (1/R, \omega_Q)$ that is traced out in frequency-momentum space relevant for the damping of the quadrupole mode is indicated by the white lines in Fig. 2a for two different atom numbers.

Compared to experiments in condensed matter systems, cold atomic gases offer unprecedented tunability of the universal system parameters, such as confinement, interaction strength, and particle number. Figure 2b–d show results for the anomalous enhancement of the shear viscosity for these different parameters evaluated at momentum $q = 1/R$ and frequency $\omega = \omega_Q$ compared to the hydrodynamic shear viscosity (i.e., evaluated at zero momentum but finite frequency). First, Fig. 2b shows the ratio of the shear viscosity as a function of the harmonic trapping frequency $\beta\omega_r$ for four interaction strengths $\ln(k_F a_2) = 0.39, 0.49, 0.56,$ and 0.63 (corresponding to chemical potentials $\beta\mu = 6.8, 7.8, 8.4, 9.0$, respectively) at fixed atom number $N = 10^3$ and temperature $T/T_F = 0.1$. On the BCS side of the crossover (i.e., for $\ln(k_F a_2) > 0$), there is a strong enhancement of the shear viscosity over the hydrodynamic result at small frequencies. As expected we observe hydrodynamic transport in the strongly interacting limit ($\ln(k_F a_2) \approx 0$) implying there is no odd-even effect. This trend continues
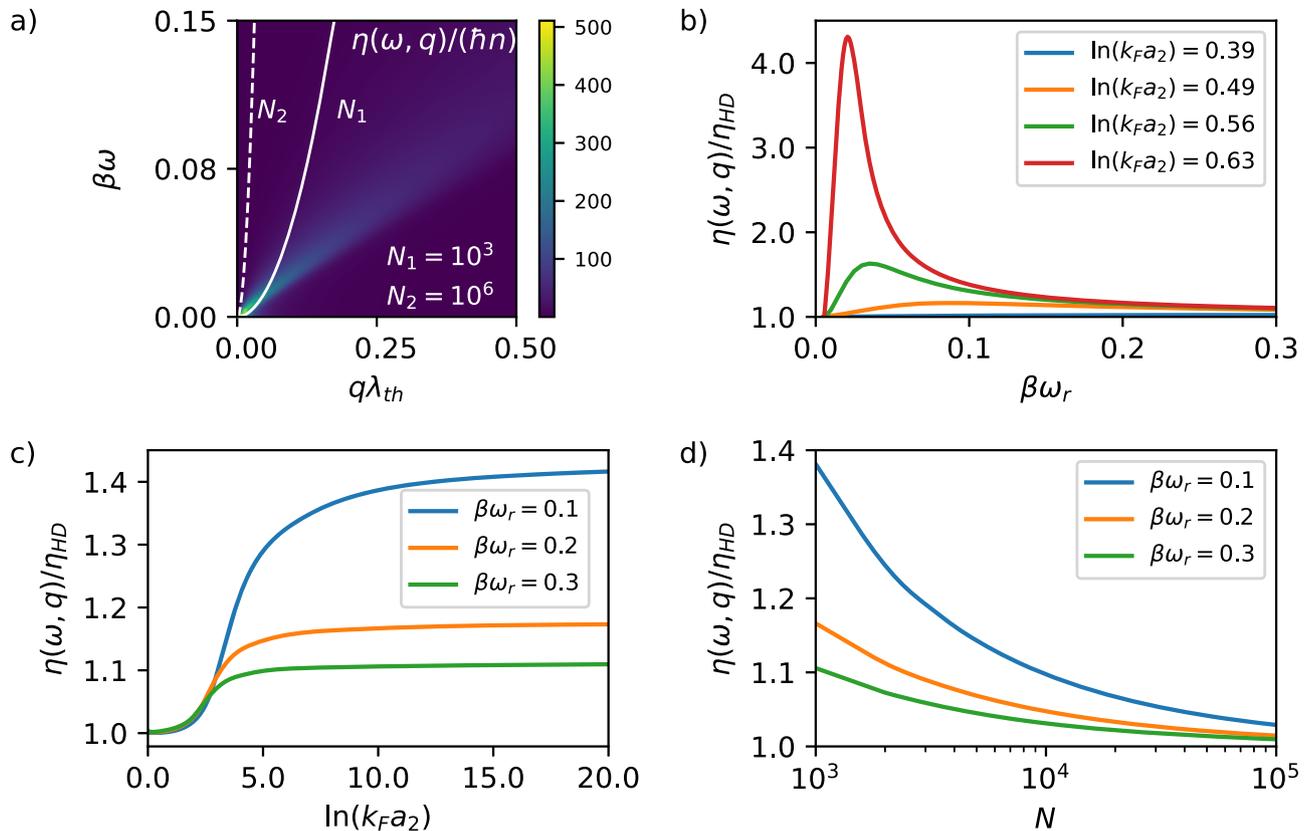
Fig. 2 | Shear viscosity spectral function and anomalous damping of the quadrupole mode. a Shear viscosity spectral function in units of $\hbar n$, where n is the particle density at the center of the harmonic trap, as a function of wave number q and frequency ω (both in thermal units with $\lambda_T = \sqrt{2\pi\beta\hbar^2/m^*}$). The white solid (dashed) line describes the path in parameter space ($q = 1/R$, $\omega = \omega_Q$) explored by tuning the trap confinement for $N_1 = 10^3$ ($N_2 = 10^6$) atoms. **b–d** Ratio of the shear viscosity spectral function $\eta(\omega = \omega_Q, q = 1/R)$ and the hydrodynamic shear viscosity

$\eta_{HD} = \eta(\omega_Q, 0)$ as a function of **b** trap frequency, **c** interaction strength, and **d** particle number. Unless otherwise specified, we use an atom number $N = 10^3$ and interaction strength $\ln(k_F a_2) = 0.63$ (corresponding to $\beta\mu = 9$). In each case, we observe a pronounced deviation from the hydrodynamic prediction for smaller atom number, interactions that are deeper in the BCS limit, and for weaker harmonic traps (or lower temperatures), respectively.

on the BEC side ($\ln(k_F a_2) < 0$) where the odd- and even-parity relaxation rates are of the same order of magnitude. This can be seen in Fig. 2c which shows the shear viscosity spectral function as a function interaction strength for three different values of the trap frequency $\beta\omega_r = 0.1, 0.2$, and 0.3, again with $N = 10^3$ particles and temperature $T/T_F = 0.1$. On the BCS side of the crossover and for finite confinement, the shear viscosity is enhanced due to the odd-even effect. The enhancement increases with increasing confinement and reduces to the hydrodynamic result for weak confinement. Finally, in Fig. 2d, we examine the shear viscosity as a function of atom number at fixed interaction strength $\ln(k_F a_2) = 0.63$ at $T/T_F = 0.1$ for three values of the trap frequency $\beta\omega_r = 0.1, 0.2$, and 0.3. Since a decreasing particle number N increases the momentum as $q = 1/R \sim N^{-1/4}$, we observe a strong enhancement for mesoscopic particle ensembles and a trend toward the hydrodynamic limit for large particle number.

Comparing these results with the criterion in Eq. (4), we indeed find that it accurately predicts the onset of the tomographic regime. As an example, for parameters where we observe an anomalous shear viscosity—such as for $\beta\omega_r = 0.1$, $\ln(k_F a) \approx 10$ and $N = 10^3$—we find $q\xi \approx 3.2$. By contrast, near resonance with $\ln(k_F a) \approx 1$ with the same $\beta\omega_r$ and N, we find $q\xi \approx 0.05$.

Discussion

We propose neutral quantum gases as a platform to observe and control the odd-even effect in quasiparticle lifetimes, which is an essential but to date unobserved fundamental aspect of Fermi liquid theory. Compared to electron Fermi liquids, neutral quantum gases offer three distinct advantages that will favor an experimental observation of the odd-even parity effect: First, the effect is widely tunable with interaction strength and vanishes on the BEC side of the crossover because the Fermi surface vanishes and Pauli blocking no longer provides a phase-space constraint for scattering. Second, the real-space confinement allows to directly access oscillatory transverse dynamics in real space and probe the shear viscosity through the damping of collective modes. While we here discuss the quadrupole mode damping in detail, in principle, one could also excite other collective modes, like the breathing mode, which is isotropic and will not depend sensitively on the odd-even effect, as a benchmark to examine the anomalous behavior of the shear viscosity. Third, the odd-even effect depends sensitively on both trap confinement and particle number and is strongly enhanced for mesoscopic Fermi gases. Although the odd-even effect will be present for any particle number as long as the temperature is sufficiently small, our findings suggest that the onset temperature of this effect increases with decreasing particle number, providing an additional way to access this effect. Already a number of experiments have been able to create mesoscopic ensembles of fermions[50–53] and would make an excellent platform for investigating this odd-even effect and its effect on the damping of the quadrupole mode.

Methods

We model the dynamics of the two-dimensional Fermi gas in the normal state using Landau's Fermi liquid theory, which describes the non-equilibrium dynamics using a kinetic equation for the fermionic quasiparticles:

$$\left[\partial_t + \frac{1}{\hbar}\nabla_{\mathbf{p}}\epsilon_{\mathbf{p}} \cdot \nabla_{\mathbf{r}} + \frac{1}{\hbar}\left(\mathcal{F} - \nabla_{\mathbf{r}}\epsilon_{\mathbf{p}}\right) \cdot \nabla_{\mathbf{p}}\right] n(\mathbf{p}) = \mathcal{I}\left[n(\mathbf{p})\right]. \quad (5)$$

Here, $n(\mathbf{p}) = n(t, \mathbf{x}, \mathbf{p})$ is the local distribution function of quasiparticles at time t and position $\mathbf{r}$ with momentum $\mathbf{p}$ (we omit the space-time dependence in the following). The quasiparticle dispersion in Eq. (5) is

$$\epsilon_{\mathbf{p}} = \frac{\hbar^2 p^2}{2m^*} + \int \frac{d\mathbf{p}'}{(2\pi)^2} f_{\mathbf{p},\mathbf{p}'} \delta n(\mathbf{p}'), \quad (6)$$

which depends on the single-particle dispersion with atomic mass m^* and a term that describes the mutual interaction energy from other quasiparticles. The interactions between quasiparticles in this term are parameterized by

$f_{\mathbf{p},\mathbf{p}'}$ and depend on $\delta n(\mathbf{p})$, the deviation of the quasiparticle distribution function away from global equilibrium. For a circular 2D Fermi surface, we expand the interaction in angular harmonics and rescale to a dimensionless form as $F_{\mathbf{p},\mathbf{p}'} = \nu f_{\mathbf{p},\mathbf{p}'} = \sum_{m=-\infty}^{\infty} F_m e^{im(\theta_{\mathbf{p}} - \theta_{\mathbf{p}'})}$, with $\nu = m^*/(\pi\hbar^2)$ the density of states at the Fermi surface, $\theta_{\mathbf{p}}$ the polar angle of the vector $\mathbf{p}$ in momentum space, and F_m the dimensionless interaction strength of the m-th harmonic. To determine the shear viscosity, we also include an external force $\mathcal{F}$ in Eq. (5) induced by a gradient of a transverse velocity field,

$$\mathcal{F}^i = m^* \mathbf{v}_{\mathbf{p}}^j \nabla_{\mathbf{r}}^i \mathbf{V}^j, \quad (7)$$

where $i, j = x, y$ are space indices, $\mathbf{v}_{\mathbf{p}} = \nabla_{\mathbf{p}}\epsilon_{\mathbf{p}}$ is the quasiparticle velocity, and $\mathbf{V}$ is a velocity field with $\nabla_{\mathbf{r}} \cdot \mathbf{V} = 0$. We impose a harmonic form of the velocity field with momentum $\mathbf{q}$ and frequency ω, i.e., $\mathbf{V} = \mathbf{V_0}e^{-i\omega t + i\mathbf{q}\cdot\mathbf{r}}$ with $\mathbf{V_0}$ a constant vector satisfying $\mathbf{q} \cdot \mathbf{V_0} = 0$.

The right-hand side of Eq. (5) is the collision integral, which describes quasiparticle relaxation due to elastic two-particle collisions,

$$\begin{aligned}\mathcal{I}[n_{\mathbf{p}}] = \frac{1}{\hbar} \int &\frac{d\mathbf{q}}{(2\pi)^2}\frac{d\mathbf{p}'}{(2\pi)^2}\frac{d\mathbf{q}'}{(2\pi)^2} |\langle\mathbf{p}', \mathbf{q}'|T|\mathbf{p}, \mathbf{q}\rangle|^2 \\ &\times (2\pi)^2\delta(\mathbf{p}+\mathbf{q}-\mathbf{p}'-\mathbf{q}')2\pi\delta\left(\epsilon_{\mathbf{p}} + \epsilon_{\mathbf{q}} - \epsilon_{\mathbf{p}'} - \epsilon_{\mathbf{q}'}\right) \\ &\times \left[(1 - n(\mathbf{p}))(1 - n(\mathbf{q}))n(\mathbf{p}')n(\mathbf{q}')\right. \\ &\left. - (\{\mathbf{p}, \mathbf{q}\} \to \{\mathbf{p}', \mathbf{q}'\})\right],\end{aligned} \quad (8)$$

where $\langle\mathbf{p}', \mathbf{q}'|T|\mathbf{p}, \mathbf{q}\rangle$ is the scattering T-matrix between states $\mathbf{p}, \mathbf{q}$ and $\mathbf{p}', \mathbf{q}'$. The linearized collision integral is then $\mathcal{L}[\psi(\mathbf{p})] = \mathcal{I}[n_{\mathbf{p}}]/[n_{\mathrm{FD}}(\mathbf{p})(1 - n_{\mathrm{FD}}(\mathbf{p}))]$ with the parameterization of Eq. (2). Within Fermi liquid theory, the T-matrix is linked to the Landau parameters F_m[7]: In terms of the dominant Landau parameter F_0 and at low temperatures, it is a function of the scaling variable $x = \omega/(v_F|\mathbf{q} - \mathbf{p}'|)$,

$$\langle\mathbf{p}', \mathbf{q}'|T|\mathbf{p}, \mathbf{q}\rangle = \frac{1}{\nu}\frac{F_0}{1 + F_0\Omega(x)}, \quad (9)$$

with the in-medium dressing function

$$\Omega(x) \approx \left[1 - \frac{x}{\sqrt{(x + i\delta)^2 - 1}}\right]\theta(\mu). \quad (10)$$

This function parametrizes repeated particle-hole scattering and is equivalent to the Lindhard function in 2D. Equation (10) holds for a well-defined Fermi surface with $\mu > 0$. In the opposite limit $\mu < 0$ (i.e., the BEC or the high-temperature limit), other processes like particle-particle scattering will be more relevant than the ones captured by Fermi liquid theory. For good measure, Supplementary Note I compares and contrasts other forms of the scattering T-matrix, which give quantitatively similar results. The dominant Landau parameter F_0 is connected to the inverse compressibility as $\kappa^{-1} = (1 + F_0)\kappa_0^{-1}$ with κ_0^{-1} the inverse compressibility of a non-interacting Fermi gas. This compressibility has been previously measured experimentally over the entire BCS-BEC crossover[36,37,54], which gives the Landau parameter F_0 in terms of the interaction parameter $\ln(k_F a_2)$. The fit is discussed in the Supplementary Note III.

We solve the kinetic equation by expanding the quasiparticle distribution function to first order in the deviation from local equilibrium, $\delta n(\mathbf{p})$, as well as the slowly varying velocity field $\mathbf{V}$. By employing a temperature-dependent eigenfunction expansion developed in[20,21], we obtain the full spectrum of eigenmodes of the collision integral $\{1/\tau_m\}$, which describe the relaxation rates of different harmonic modes. In addition, this procedure allows for an exact solution of the linearized Boltzmann equation $\delta n(\mathbf{p})$ in response to the shear flow $\mathbf{V}$. The solution of $\delta n(\mathbf{p})$ then

gives the linear response of the off-diagonal elements of the stress tensor,

$$\Pi^{xy} = \int \frac{d\mathbf{p}}{(2\pi)^2} m^* v_{p_x} v_{p_y} \delta n(\mathbf{p}) \approx i\eta(\omega, q) q_x V_y^0, \tag{11}$$

from which we compute the shear viscosity spectral function $\eta(\omega, q)$.

Data availability
The raw data for the figures are available upon request, addressed to any of the authors.

Code availability
Requests should be addressed to any of the authors.

References
1. Sommerfeld, A. Zur Elektronentheorie der Metalle auf Grund der Fermischen Statistik, I. Teil. *Zeit. Phys.* **47**, 1 (1928).
2. Sommerfeld, A. Zur Elektronentheorie der Metalle auf Grund der Fermischen Statistik, II. Teil. *Zeit. Phys.* **47**, 43 (1928).
3. Landau, L. D. The theory of a Fermi liquid. *Sov. Phys. JETP* **3**, 920 (1957).
4. Landau, L. D. Oscillations in a Fermi liquid. *Sov. Phys. JETP* **5**, 101 (1957).
5. Pines, D. and Nozières, P. *The Theory of Quantum Liquids.* CRC Press. https://doi.org/10.1201/9780429495717 (Boca Raton, 2018).
6. Giuliani, G. and Vignale, G. *Quantum Theory of the Electron Liquid*, Cambridge University Press. https://doi.org/10.1017/CBO9780511619915 (Cambridge, 2005).
7. Baym, G. and Pethick, C. *Landau Fermi Liquid Theory: Concepts and Applications*, Wiley-VCH Verlag. https://doi.org/10.1002/9783527617159 (Weinheim, 2004).
8. Schirotzek, A., Wu, C.-H., Sommer, A. & Zwierlein, M. W. Observation of Fermi polarons in a tunable Fermi liquid of ultracold atoms. *Phys. Rev. Lett.* **102**, 230402 (2009).
9. Nascimbène, S. et al. Collective oscillations of an imbalanced fermi gas: axial compression modes and polaron effective mass. *Phys. Rev. Lett.* **103**, 170402 (2009).
10. Scazza, F. et al. Repulsive fermi polarons in a resonant mixture of ultracold ^{6}Li atoms. *Phys. Rev. Lett.* **118**, 083602 (2017).
11. Yan, Z. et al. Boiling a unitary Fermi liquid. *Phys. Rev. Lett.* **122**, 093401 (2019).
12. Nascimbène, S., Navon, N., Jiang, K. J., Chevy, F. & Salomon, C. Exploring the thermodynamics of a universal Fermi gas. *Nature* **463**, 1057 (2010).
13. Ku, M. J. H., Sommer, A. T., Cheuk, L. W. & Zwierlein, M. W. Revealing the superfluid lambda transition in the universal thermodynamics of a unitary Fermi gas. *Science* **335**, 563 (2012).
14. Vogt, E. et al. Scale invariance and viscosity of a two-dimensional fermi gas. *Phys. Rev. Lett.* **108**, 070404 (2012).
15. Patel, P. B. et al. Universal sound diffusion in a strongly interacting Fermi gas. *Science* **370**, 1222 (2020).
16. Huang, S. et al. Emergence of sound in a tunable fermi fluid. *Phys. Rev. X* **15**, 011074 (2025).
17. Wenz, A. N. et al. From few to many: observing the formation of a Fermi sea one atom at a time. *Science* **342**, 457 (2013).
18. Ledwith, P. J., Guo, H. & Levitov, L. The hierarchy of excitation lifetimes in two-dimensional Fermi gases. *Ann. Phys.* **411**, 167913 (2019).
19. Ledwith, P., Guo, H., Shytov, A. & Levitov, L. Tomographic dynamics and scale-dependent viscosity in 2D electron systems. *Phys. Rev. Lett.* **123**, 116601 (2019).
20. Hofmann, J. & Gran, U. Anomalously long lifetimes in two-dimensional Fermi liquids. *Phys. Rev. B* **108**, L121401 (2023).
21. Nilsson, E., Gran, U. and Hofmann, J. Nonequilibrium relaxation and odd-even effect in finite-temperature electron gases, *arXiv preprint arXiv:2405.03635* (2024).
22. Fritz, L. & Scaffidi, T. Hydrodynamic electronic transport. *Annu. Rev. Condens. Matter Phys.* **15**, 17–44 (2024).
23. Hofmann, J. & Das Sarma, S. Collective modes in interacting two-dimensional tomographic Fermi liquids. *Phys. Rev. B* **106**, 205412 (2022).
24. Hofmann, J. & Rostami, H. Nonlinear thermoelectric probes of anomalous electron lifetimes in topological fermi liquids. *Phys. Rev. Res.* **6**, L042042 (2024).
25. Nazaryan, K. G. & Levitov, L. Nonlocal conductivity, continued fractions, and current vortices in electron fluids. *Phys. Rev. B* **110**, 045147 (2024).
26. Estrada-Álvarez, J. et al. Superballistic conduction in hydrodynamic antidot graphene superlattices. *Phys. Rev. X* **15**, 011039 (2025).
27. Zeng, Y. et al. Quantitative measurement of viscosity in two-dimensional electron fluids. *arXiv preprint arXiv:2407.05026* (2024).
28. Roach, P. R. & Ketterson, J. B. Observation of transverse zero sound in normal ^{3}He. *Phys. Rev. Lett.* **36**, 736 (1976).
29. Flowers, E. G., Richardson, R. W. & Williamson, S. J. Transverse zero sound in normal ^{3}He. *Phys. Rev. Lett.* **37**, 309 (1976).
30. Chin, C., Grimm, R., Julienne, P. & Tiesinga, E. Feshbach resonances in ultracold gases. *Rev. Mod. Phys.* **82**, 1225 (2010).
31. Haller, E. et al. Confinement-induced resonances in low-dimensional quantum systems. *Phys. Rev. Lett.* **104**, 153203 (2010).
32. Gran, U., Nilsson, E. and Hofmann, J. Shear viscosity in interacting two-dimensional Fermi liquids, *arXiv preprint arXiv:2312.09977* (2023).
33. Frank, B., Zwerger, W. & Enss, T. Quantum critical thermal transport in the unitary Fermi gas. *Phys. Rev. Res.* **2**, 023301 (2020).
34. Dolgirev, P. E. et al. Accelerating analysis of Boltzmann equations using Gaussian mixture models: application to quantum Bose-Fermi mixtures. *Phys. Rev. Res.* **6**, 033017 (2024).
35. Baur, S. K., Vogt, E., Köhl, M. & Bruun, G. M. Collective modes of a two-dimensional spin-1/2 Fermi gas in a harmonic trap. *Phys. Rev. A* **87**, 043612 (2013).
36. Makhalov, V., Martiyanov, K. & Turlapov, A. Ground-state pressure of quasi-2D Fermi and Bose gases. *Phys. Rev. Lett.* **112**, 045301 (2014).
37. Boettcher, I. et al. Equation of state of ultracold fermions in the 2D BEC-BCS crossover region. *Phys. Rev. Lett.* **116**, 045303 (2016).
38. Hueck, K. et al. Two-dimensional homogeneous Fermi gases. *Phys. Rev. Lett.* **120**, 060402 (2018).
39. Ghosh, T. & Sinha, S. Splitting between quadrupole modes of dilute quantum gas in a two-dimensional anisotropic trap. *Eur. Phys. J. D* **19**, 371 (2002).
40. Bulgac, A. & Bertsch, G. F. Collective oscillations of a trapped Fermi gas near the unitary limit. *Phys. Rev. Lett.* **94**, 070401 (2005).
41. Klimin, S. N., Tempere, J., Devreese, J. T. & Van Schaeybroeck, B. Collective modes of an imbalanced trapped Fermi gas in two dimensions at finite temperatures. *Phys. Rev. A* **83**, 063636 (2011).
42. Enss, T., Küppersbusch, C. & Fritz, L. Shear viscosity and spin diffusion in a two-dimensional Fermi gas. *Phys. Rev. A* **86**, 013617 (2012).
43. Bruun, G. M. Shear viscosity and spin-diffusion coefficient of a two-dimensional Fermi gas. *Phys. Rev. A* **85**, 013636 (2012).
44. Schäfer, T. Shear viscosity and damping of collective modes in a two-dimensional Fermi gas. *Phys. Rev. A* **85**, 033623 (2012).
45. Chiacchiera, S., Davesne, D., Enss, T. & Urban, M. Damping of the quadrupole mode in a two-dimensional Fermi gas. *Phys. Rev. A* **88**, 053616 (2013).
46. Chafin, C. & Schäfer, T. Scale breaking and fluid dynamics in a dilute two-dimensional Fermi gas. *Phys. Rev. A* **88**, 043636 (2013).

47. Hofmann, J., Chevy, F., Goulko, O. & Lobo, C. Collective modes of an imbalanced unitary Fermi gas. *Phys. Rev. A* **97**, 033613 (2018).

48. Bradlyn, B., Goldstein, M. & Read, N. Kubo formulas for viscosity: Hall viscosity, Ward identities, and the relation with conductivity. *Phys. Rev. B* **86**, 245309 (2012).

49. Khoo, J. Y. & Villadiego, I. S. Shear sound of two-dimensional fermi liquids. *Phys. Rev. B* **99**, 075434 (2019).

50. Peppler, T. et al. Quantum anomaly and 2D-3D crossover in strongly interacting Fermi gases. *Phys. Rev. Lett.* **121**, 120402 (2018).

51. Sobirey, L. et al. Observing the influence of reduced dimensionality on fermionic superfluids. *Phys. Rev. Lett.* **129**, 083601 (2022).

52. Brandstetter, S. et al. Emergent interaction-driven elliptic flow of few fermionic atoms. *Nat. Phys.* **21**, 52 (2025).

53. Verstraten, J. et al. In-situ imaging of a single-atom wave packet in continuous space, *arXiv preprint 2404.05699* (2024).

54. Fenech, K. et al. Thermodynamics of an attractive 2D fermi gas. *Phys. Rev. Lett.* **116**, 045302 (2016).

Author contributions
J.M., U.G., and J.H. all contributed equally to the conception, computations, and preparation of the manuscript.

Competing interests
The authors declare no competing interests.

Additional information
Supplementary information The online version contains supplementary material available at https://doi.org/10.1038/s42005-025-02231-w.

Correspondence and requests for materials should be addressed to Jeff Maki, Ulf Gran or Johannes Hofmann.

Peer review information *Communications Physics* thanks the anonymous reviewers for their contribution to the peer review of this work.

Reprints and permissions information is available at http://www.nature.com/reprints

Publisher's note Springer Nature remains neutral with regard to jurisdictional claims in published maps and institutional affiliations.